P-03-85

Forsmark site investigation

KFM01A: RVS model of fractures

Prediction of sections for stress measurements in KFM01B

Isabelle Staub, Golder Associates AB

September 2003

Svensk Kärnbränslehantering AB
Swedish Nuclear Fuel
and Waste Management Co
Box 5864
SE-102 40 Stockholm Sweden
Tel 08-459 84 00
+46 8 459 84 00
Fax 08-661 57 19
+46 8 661 57 19

ISSN 1651-4416
SKB P-03-85

Forsmark site investigation

KFM01A: RVS model of fractures

Prediction of sections for stress measurements in KFM01B

Isabelle Staub, Golder Associates AB

September 2003

This report concerns a study which was conducted for SKB. The conclusions and viewpoints presented in the report are those of the author and do not necessarily coincide with those of the client.

A pdf version of this document can be downloaded from www.skb.se

Contents

1 Introduction

A borehole KFM01B is planned to be drilled at proximity of the existing borehole KFM01A. The aim is to perform stress measurements in the planned borehole. This report aims to predict fracturing in KFM01B based on observed fractures in KFM01A. RVS has been used to visualise sections of KFM01A at the depths –250, –400 and –500m.

The predictions in KFM01B are based mostly on observations and analysis of fracture orientation and density in borehole KFM01A as well as general expertise. A general presentation of the fracturing in KFM01A is provided in section 2. The identification of the 3 depth sections targeted for stress measurements is presented in section 3.

2 Description of the model

2.1 Presentation of input data

The model is built in the master coordinate system RT90-RH70. The geometry of the drilled and planned boreholes, respectively called KFM01A and KFM01B, is found in Table 2-1. The relative localisation in space of both boreholes is illustrated in Figure 2-1.

The model has been built in order to visualise sealed and natural fractures along borehole KFM01A. The 3D model facilitates the observation of fracture orientation and gives a support for the interpretation of potential fracturing in the planned borehole KFM01B.

Data used for building the model are orientation data (strike and dip) for natural and sealed fractures in KFM01A, which are extracted from SKB's database Sicada.

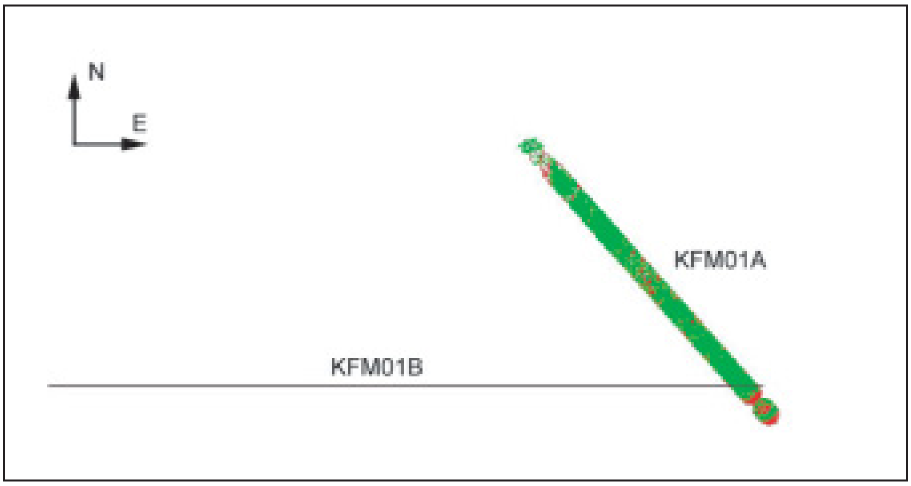

Figure 2-1. *Localisation of boreholes KFM01A and KFM01B. Top view. Fractures are visualised as discs along KFM01A (green: sealed fractures; red: natural fractures).*

Table 2-1. Geometry of the boreholes used for the development of the model.

	Start point					
	Easting, m	**Northing, m**	**Depth, m**	**Bearing**	**Inclination**	**Length, m**
KFM01A	1631397.16	6699529.813	3.125	318.352	–84.734	1001.45
KFM01B	1631394	6699539	3.15	270	–80	> 500 m

2.2 Analysis of fracturing in KFM01A

A preliminary analysis of the orientation of natural fractures mapped in KFM01A shows that sub-horizontal fractures dominate the fracture pattern, see Figure 2-2. One other important fracture set is formed by sub-vertical fractures striking NE. Three subordinates fracture sets can also be identified, that are striking ENE, N and NNW and dipping respectively 70–80°, 70–80° and 40–50°.

The same analysis performed on sealed fractures illustrates one clearly dominant fracture set striking NE and steeply dipping (75–90°), see Figure 2-3. Two subordinate sets are also identified that are striking N and ENE and dipping respectively 80–90° and 60–70°. These sets show similar orientations as those identified for natural fractures.

The spatial distribution of fractures along the borehole mostly appears in "swarms", i.e sections of boreholes show high fracture frequency which passes over to sections of lower fracture frequency and even quite long sections without any observed fractures, see Figure 2-4.

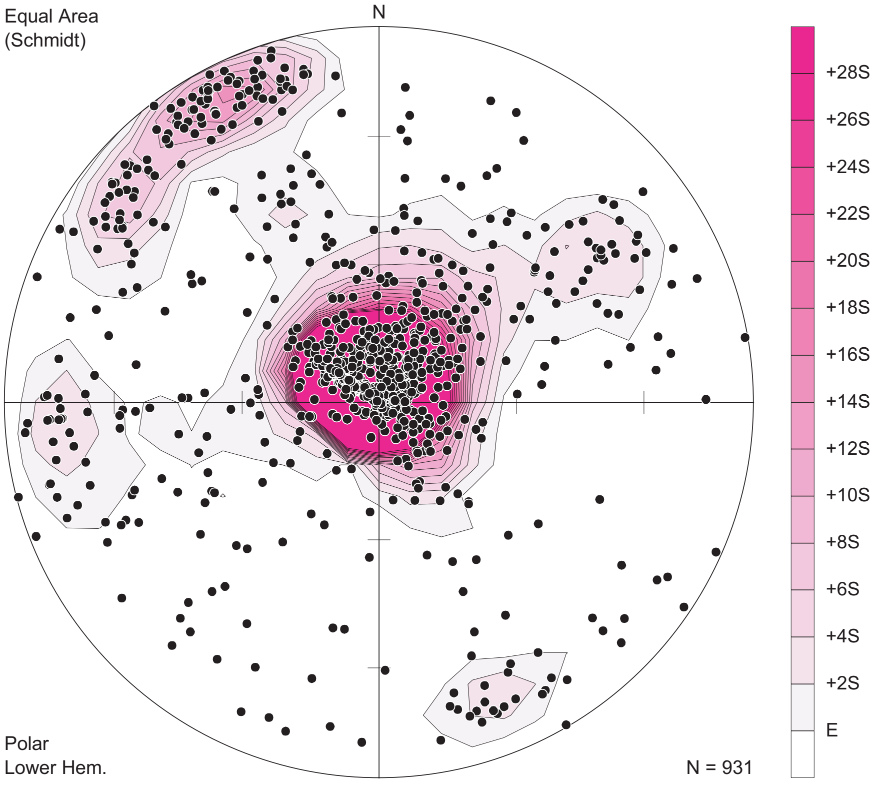

***Figure 2-2.** Lower hemisphere equal area stereoprojection of poles to natural fractures in KFM01A.*

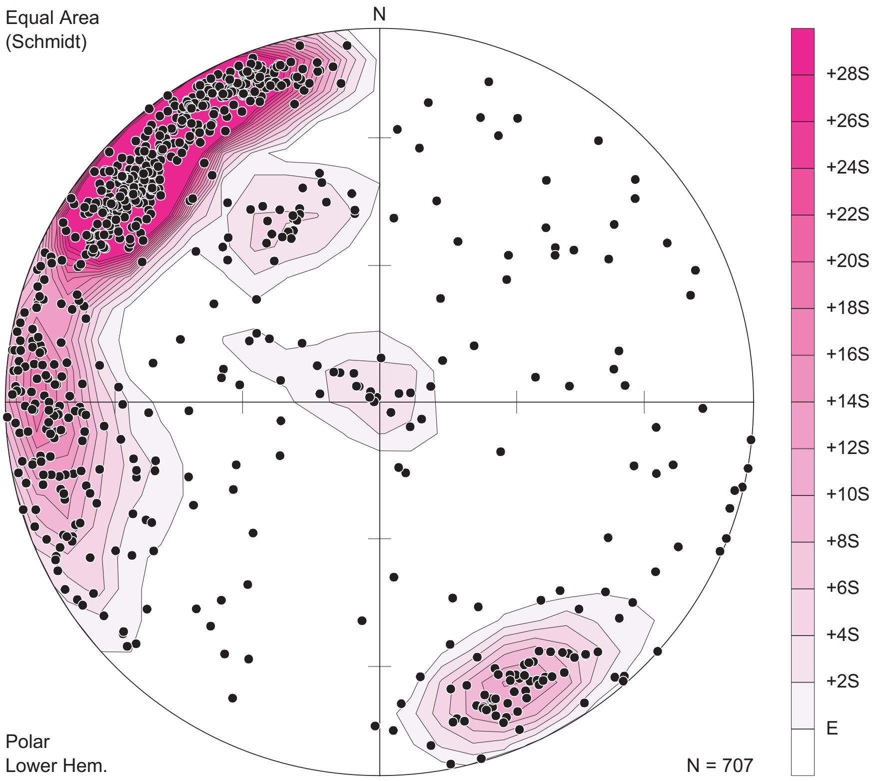

***Figure 2-3.** Lower hemisphere equal area stereoprojection of poles to sealed fractures in KFM01A.*

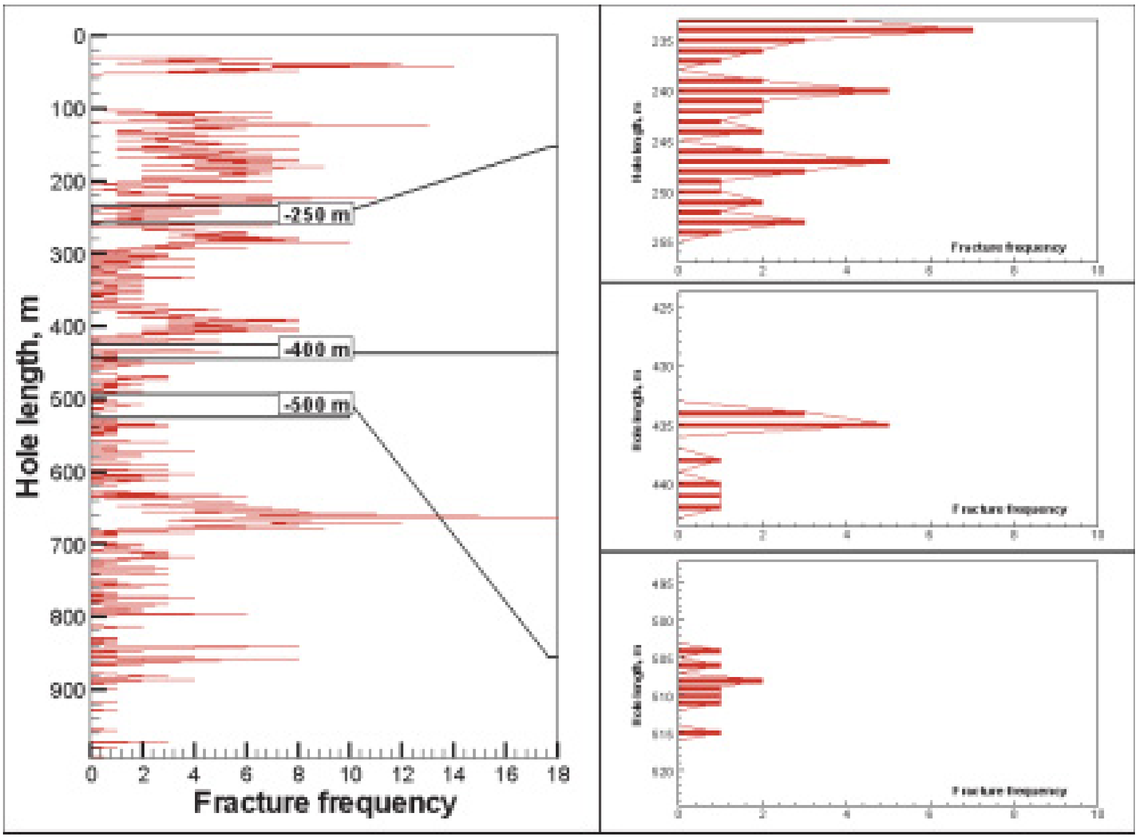

***Figure 2-4.** Fracture frequency diagram for borehole KFM01A. Details on the target sections.*

3 Description of the target sections in KFM01B

3.1 Assumptions

Some assumptions are made in order to build the model and extrapolate fracturing information from KFM01A to KFM01B.

- The choice of sections in KFM01B is based on fracture orientation and fracture spacing pattern in KFM01A. The investigated sections in KFM01A were predefined by SKB.
- Despite the quite significant distance between KFM01A and KFM01B at the targeted depths, the fracturing pattern in KFM01B has been based on deterministic study of fracturing in KFM01A.
- The fracture sets striking N, NE and ENE are sub-vertical or steeply dipping. The extrapolation of these fractures from KFM01A to KFM01B is considered being highly uncertain with regards to the relative position and distance between both boreholes and the probable realistic fracture length.
- We assume that the fracturing pattern observed in KFM01A would mirror the expected fracturing in KFM01B. We might expect the same pattern of spatial distribution of fractures.

3.2 General presentation of the sections

The depths chosen at first for the measurements in KFM01B are: –250, –400 and –500 m. We investigated the fracturing in 50–100 m windows around these depths in KFM01A. The distances between both boreholes are respectively 30–35 m, 50–55 m, and 65–70 m (Figure 3-1).

The investigated sections in KFM01A were divided in smaller segments based on the intensity of fracturing (Table 3-1). The targeted areas in the planned borehole KFM01B are those showing low fracture frequency. The following sections of the report present a detailed description of each target sections at the three depths.

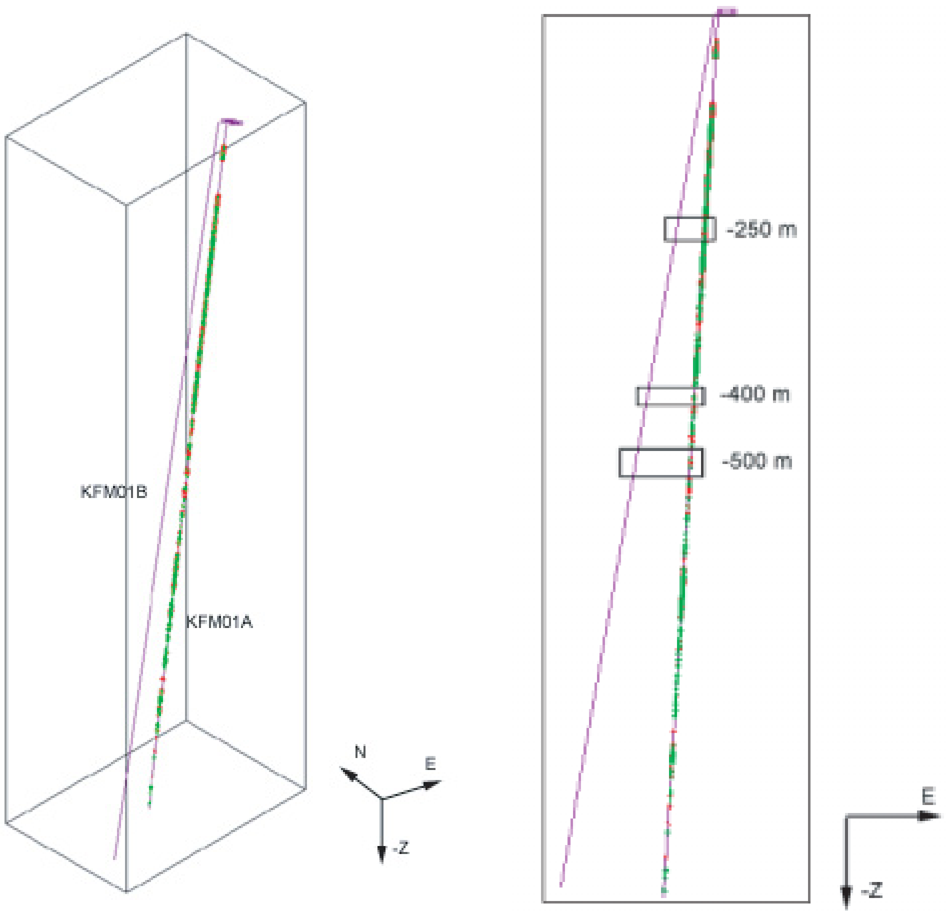

Figure 3-1. *Localisation of both boreholes and illustration of the distance between both objects at depth. Fractures are visualised as discs along KFM01A (green: sealed fractures; red: natural fractures).*

Table 3-1. Analysis of fracturing in the different target sections.

Length along KFM01B, m	"Mean" fracture spacing, m Natural fractures Sub-horizontal	Steep	Sealed fractures Sub-horizontal	Steep
236–250	0.5–1.5	0.15–1	–	0.1–4.7
250–255	0.7	0.5–1	–	0.5
255–260	– (1 fracture)	–	–	–
430–437	–	–	–	–
437–450	3.5	0.15–0.5	–	0.15–5
500–510	–	–	–	–
510–522	1	–	–	8.5
522–532	–	–	–	–

3.3 Prediction of the fracturing in the –250 m section in KFM01B

We assume that the fracturing in KFM01A in the section –250 m is completely reflected in KFM01B.

The fracturing in KFM01A at this depth shows that the top of the section is situated just below a high fracture frequency section. Based on the fracturing pattern (the fracture spacing and orientation) observed in KFM01A along this section the target length can be divided in three sub-sections (Figure 3-2 and Figure 3-3):

- Between 236 and 250 m along KFM01B: the fracture frequency is still significant, natural fractures are dominated by sub-horizontal orientation with around 1m spacing. Other natural fractures are striking NNW and dipping 70–80°. Sealed fractures are mostly steeply dipping (70–80°) and striking NNW besides two striking NE.
- Between 250 and 255 m along KFM01B: few natural fractures and only 2 sealed fractures. The natural fractures are either sub-horizontal or striking ENE. The sealed fractures are striking N and steeply dipping (80–90°).
- Between 255 and 260 m along KFM01B: only one natural fracture is mapped. A picture of this section of the core is shown in appendix 1.

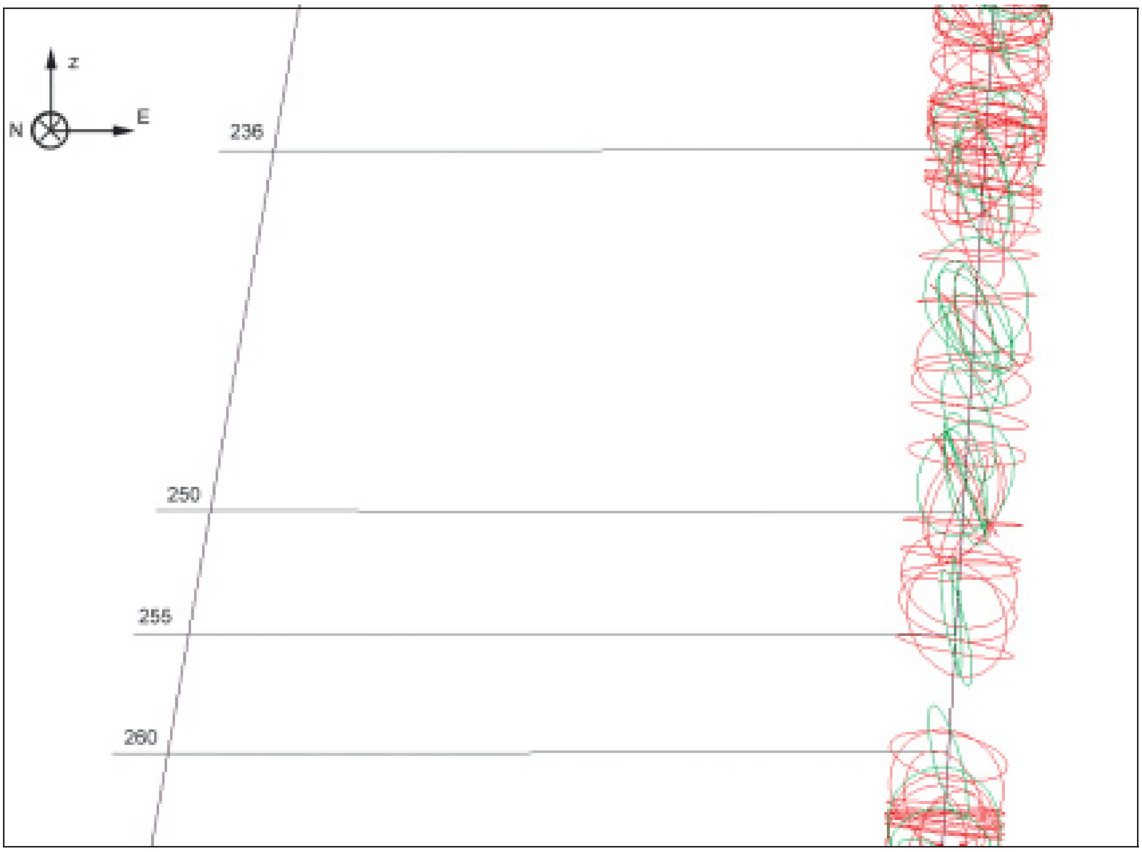

Figure 3-2. *Illustration of the –250 m section. Fractures are visualised as discs along KFM01A (red: natural fractures, green: sealed fractures).*

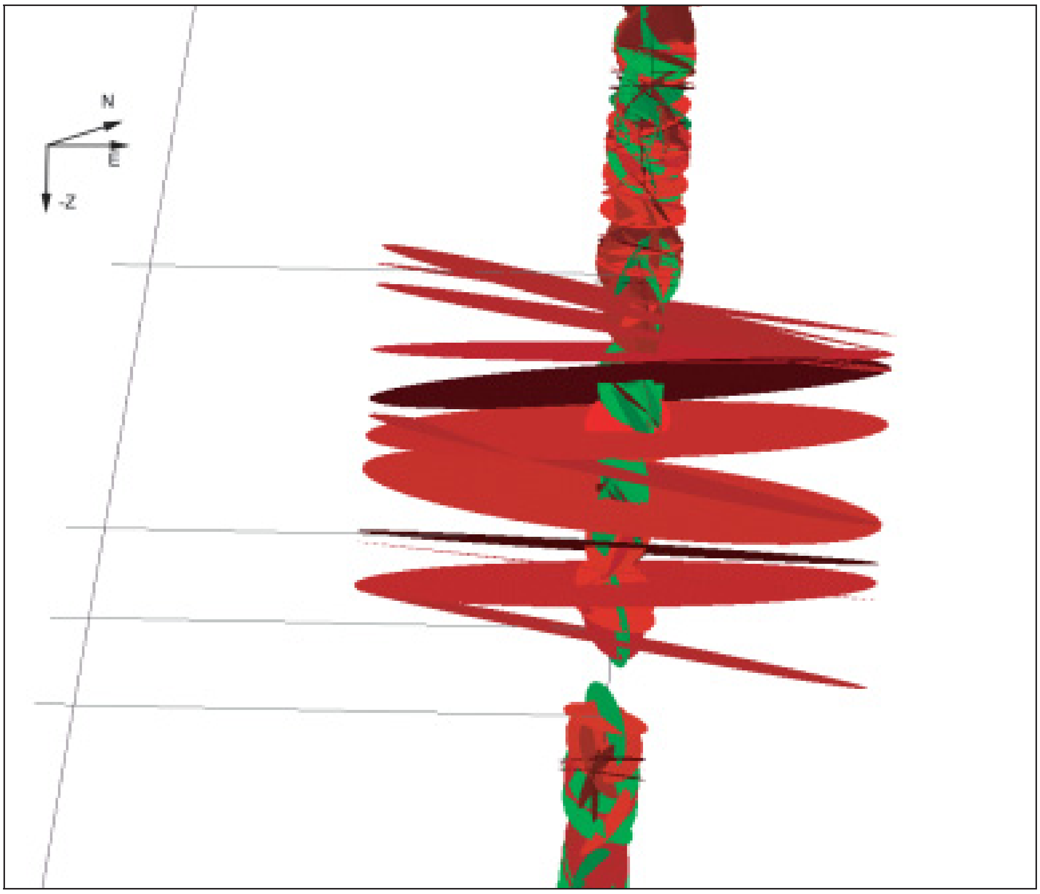

Figure 3-3. Illustration of the –250 m section. Fractures are visualised as discs along KFM01A (red: natural fractures, green: sealed fractures). Sub-horizontal fractures are visualised with larger discs.

3.4 Prediction of the fracturing in the –400 m section in KFM01B

We assume that the fracturing in KFM01A in the section –400 m is completely reflected in KFM01B.

The fracturing in KFM01A at this depth shows that the top of the section is situated just below a high fracture frequency section, especially regarding sealed fractures. Based on the fracturing pattern (fracture spacing and orientation) observed in KFM01A along this section the target length can be divided in two sub-sections (Figure 3-4 and Figure 3-5):

- Between 430 and 437 m along KFM01B: no fractures mapped. A picture of this section of the core is shown in appendix 2.
- Between 437 and 450 m along KFM01B: very low fracture frequency, natural fractures appear in swarm at the top of the section (4 fractures in the first 6 meters), 2 swarms of sealed fractures, the second are fractures striking N and sub-vertical. The upper swarm is composed of steeply dipping fractures striking NE.

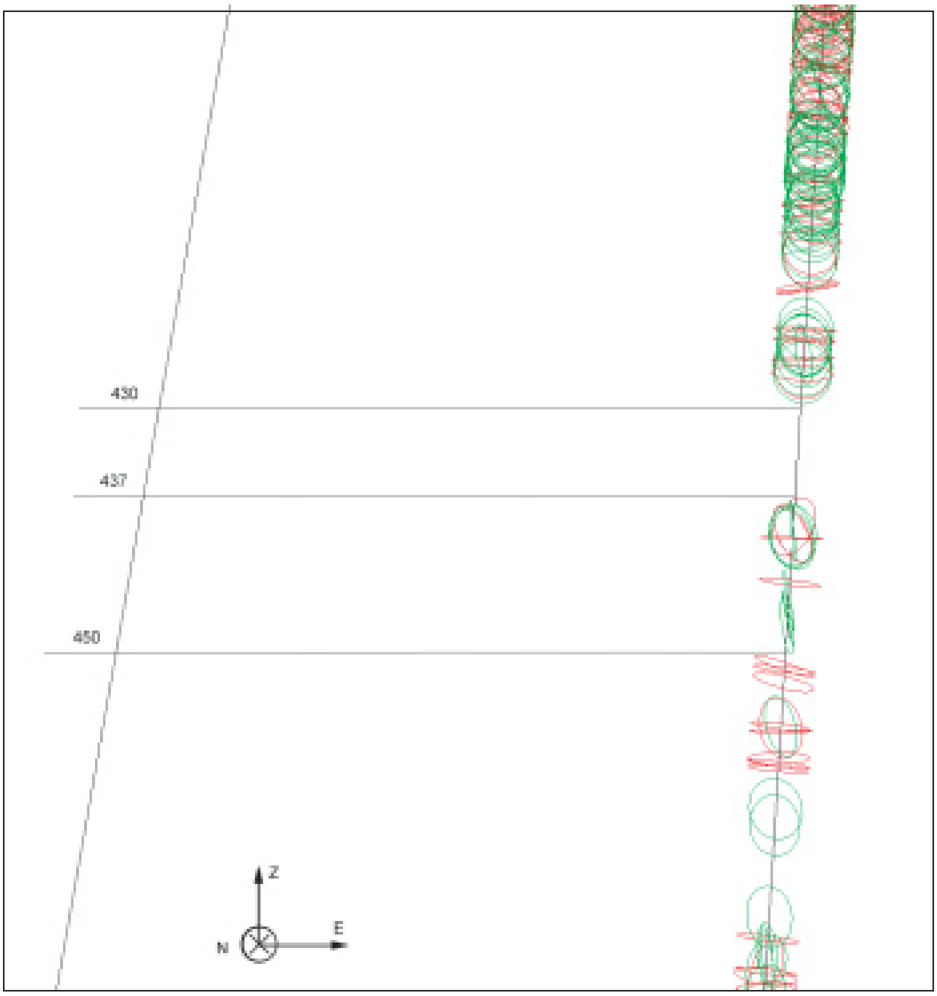

Figure 3-4. *Illustration of the –400 m section. Fractures are visualised as discs along KFM01A (red: natural fractures, green: sealed fractures).*

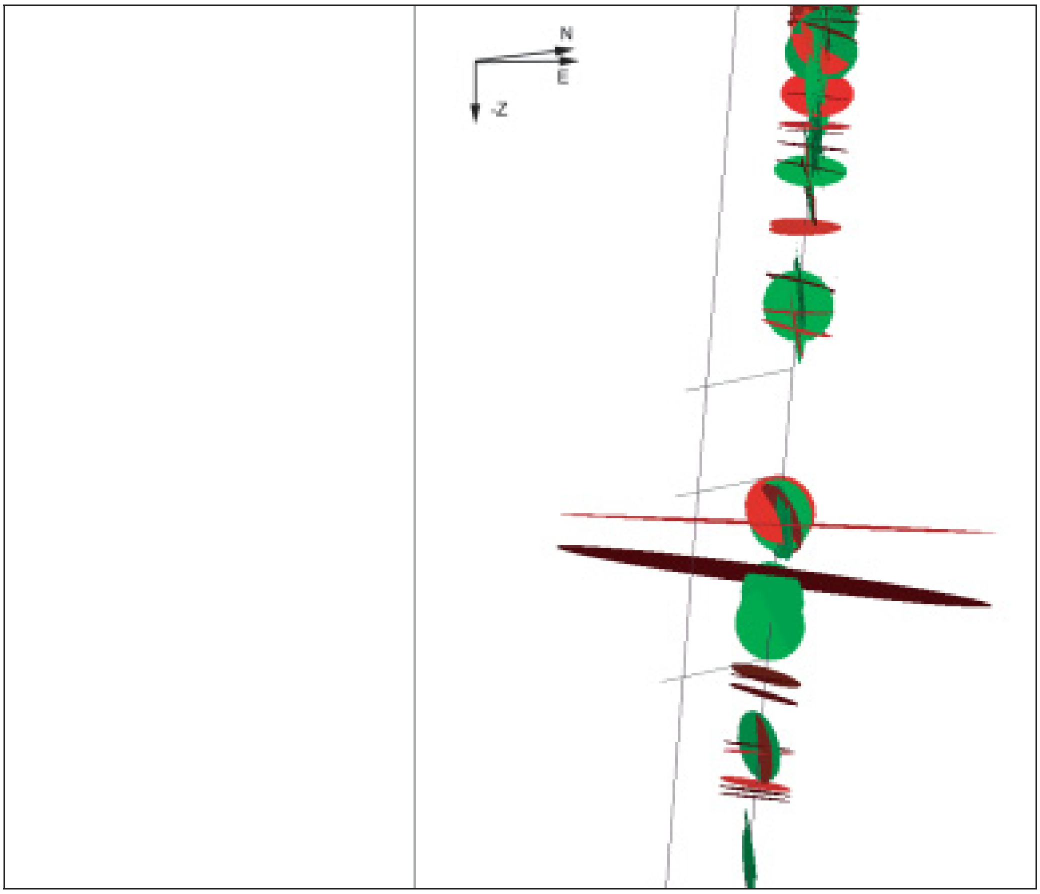

Figure 3-5. *Illustration of the –400 m section. Fractures are visualised as discs along KFM01A (red: natural fractures, green: sealed fractures). Sub-horizontal fractures are visualised with larger discs.*

3.5 Prediction of the fracturing in the –500 m section in KFM01B

We assume that the fracturing in KFM01A in the section –500 m is completely reflected in KFM01B.

The fracturing in KFM01A at this depth shows that the top of the section is situated below a swarm section of medium fracture frequency. Based on the fracturing pattern (fracture spacing and orientation) observed in KFM01A along this section the target length can be divided in three sub-sections (Figure 3-6 and Figure 3-7):

- Between 500 and 510 m along KFM01B: no fractures mapped.
- Between 510 and 522 m along KFM01B: sparse fracturing, mostly represented by sub-horizontal natural fractures. Only two sealed fractures, gently dipping (45°) and striking NE and NW.
- Between 522 and 532 m along KFM01B: no fractures mapped.

Pictures of both sections of the core without any fractures mapped are shown in appendix 3. The photos illustrate and confirm the very good quality of the core.

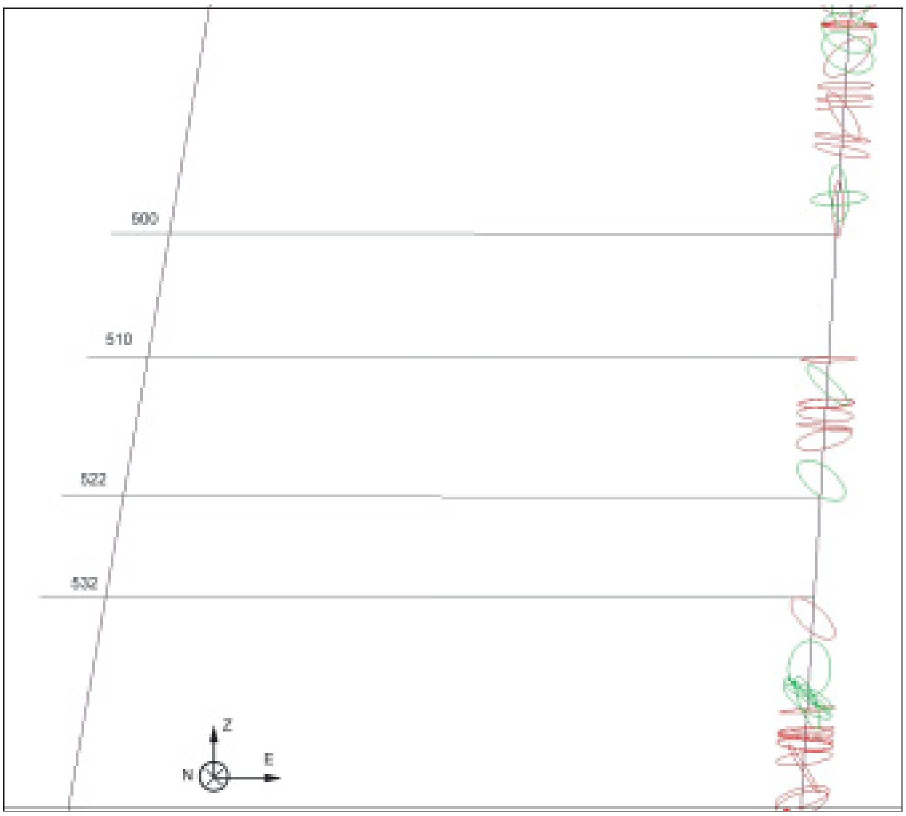

Figure 3-6. *Illustration of the –500 m section. Fractures are visualised as discs along KFM01A (red: natural fractures, green: sealed fractures).*

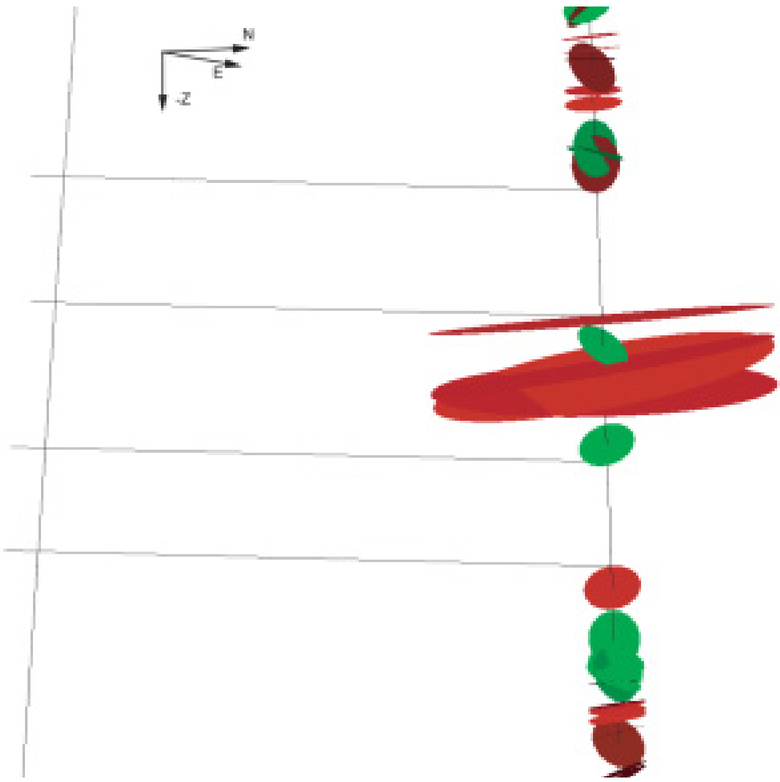

Figure 3-7. *Illustration of the –500 m section. Fractures are visualised as discs along KFM01A (red: natural fractures, green: sealed fractures). Sub-horizontal fractures are visualised with larger discs.*

4 Conclusions

The model of fracturing developed in KFM01B is based on fracture pattern (orientation and spacing) observed for natural and sealed fractures in KFM01A. The target sections at different depths have been described on the basis of information provided at the same depths in KFM01A. "Coarse" assumptions have been made to extrapolate the characteristics of fracturing from KFM01A to KFM01B especially in regards to the distance between both boreholes that increases with depth, see Figure 4-1.

The analysis of fracture trace lengths on lineaments data in the domain defined for the site investigation, and in which the boreholes are located, leads to a definition of the distribution of fracture size. Fracture size is found to follow a Power law distribution with a fractal dimension D between 2.8 and 3 for the different fracture sets.

Based on this equation the Cumulative Density Function for fracture size in this area can be calculated and the resulting curve is illustrated in Figure 4-2. The minimum and maximum cut-off lengths are set to 0.2 respectively 400 m. According to this graph 99% of the fractures are estimated to be smaller than 3m equivalent radius and the probability of fractures larger than 10 m equivalent radius is almost zero. Hence the probability of predicting fractures in KFM01B based on fracture pattern in KFM01A is almost zero.

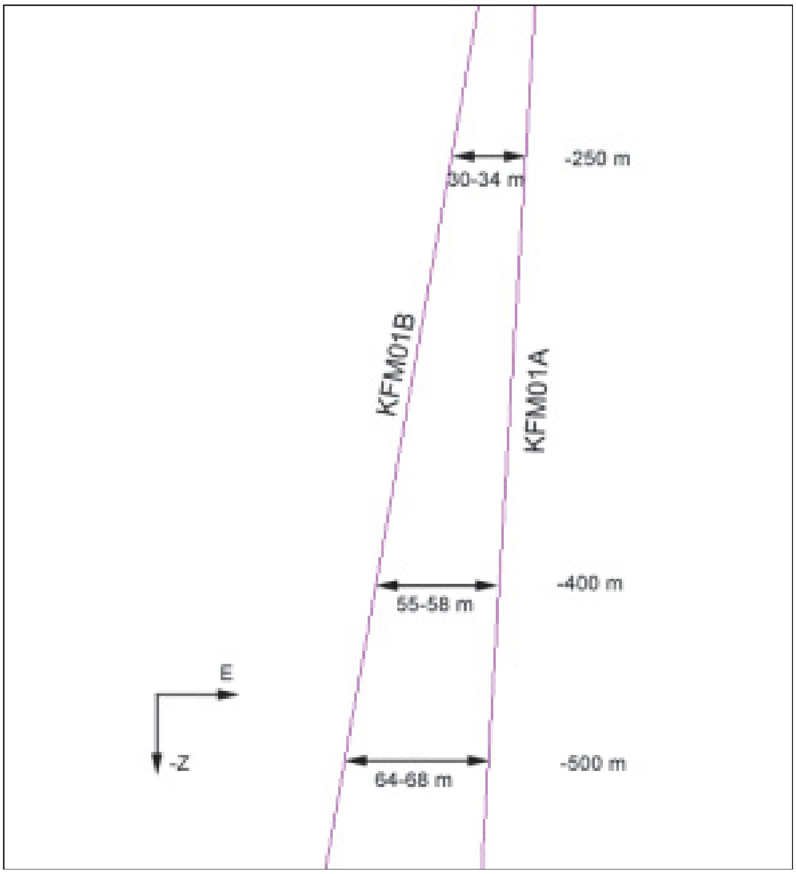

Figure 4-1. *Evaluation of the distance between both boreholes at the depth of the targeted sections.*

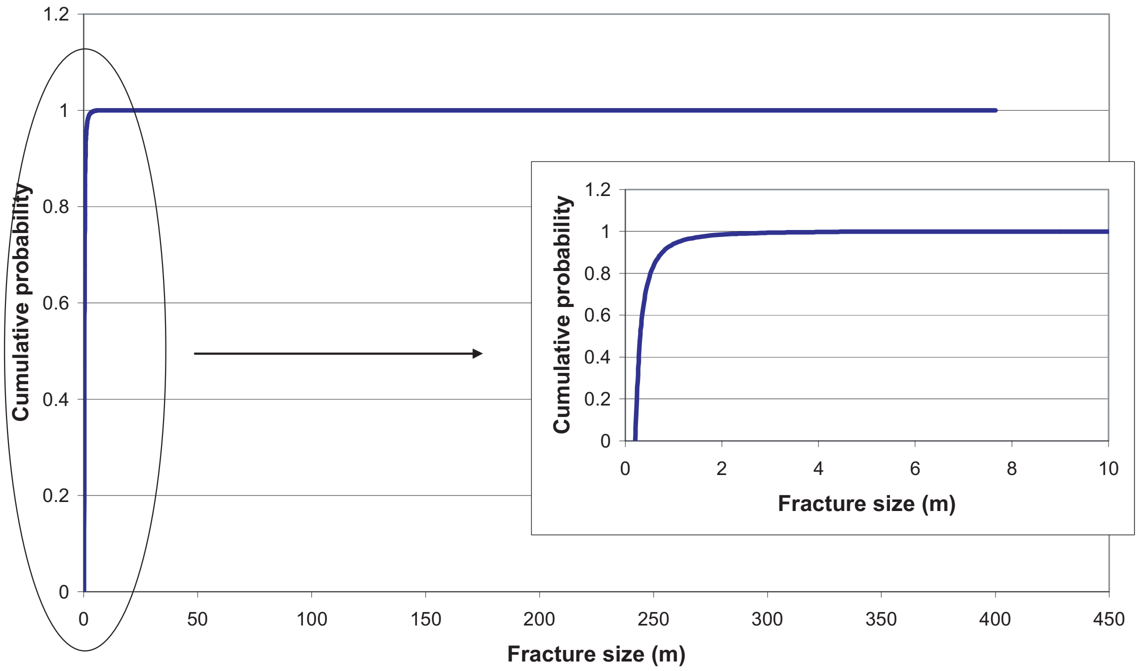

Figure 4-2. *"Theoretical" fracture length distribution, based on parameters for fracture set NE.*

As a consequence the model is not based on predictions of fractures by elongation of existing fractures in KFM01A towards their intersection points in KFM01B, but on the fracture pattern in KFM01A and the assumption that the same fracture pattern at comparable depths might be found in KFM01B.

From the developed model three sections of 20–30 m length have been identified in KFM01B. Based on the description of these depth sections in KFM01A some significant fracture free or low fracture frequency sections are expected in these intervals.

Photos of the KFM01A core – section –250 m

Picture A1-1. *Core of KFM01A, lower segment of the –250 m section (at Length 253–257 m along KFM01A).*

Appendix 2

Photos of the KFM01A core – section –400 m

Picture A2-1. *Core of KFM01A, upper segment of the –400 m section (at Length 424–431 m along KFM01A).*

Appendix 3

Photos of the KFM01A core – section –500 m

Picture A3-1. *Core of KFM01A, upper segment of the –500 m section (at Length 492–501.54 m along KFM01A).*

Picture A3-2. *Core of KFM01A, upper segment of the –500 m section (at Length 501.54–503 m along KFM01A).*

Picture A3-3. *Core of KFM01A, lower segment of the –500 m section (at Length515.7–524.14 m along KFM01A).*

Picture A3-4. *Core of KFM01A, lower segment of the –500 m section (at Length 524.14–524.8 m along KFM01A).*